Unusual Isomeric Lability in Both Oxidation States of the Redox Systems *fac*-/*mer*-$[M(CO)_3(\eta^3\text{-}P_2P')]^+/M(CO)_3(\eta^3\text{-}P_2P')$ (M = Cr, Mo, W; P_2P' = Bis(2-(diphenylphosphino)ethyl)phenylphosphine): The First Examples Where the 17-Electron *fac*$^+$ and *mer*$^+$ Isomers Are of Comparable Stability

Alan M. Bond,*[1] Ray Colton,*[2] Stephen W. Feldberg,[1,3] Peter J. Mahon,[1] and Tania Whyte[2]

Department of Chemical and Analytical Sciences, Deakin University, Geelong, Victoria 3217, Australia, and Inorganic Chemistry Section, School of Chemistry, University of Melbourne, Parkville, Victoria 3052, Australia

Received December 28, 1990

Oxidative cyclic voltammetric experiments have been carried out in dichloromethane solution on the sterically strained 18-electron $M(CO)_3(\eta^3\text{-}P_2P')$ complexes (M = Cr, Mo, W; P_2P' = $Ph_2PCH_2CH_2P(Ph)CH_2CH_2PPh_2$). A wide range of scan rates (0.01–8000 V s^{-1}) and temperatures (+20 to −60 °C) have been used at both conventional and micro platinum-disk electrodes to establish the mechanism of the one-electron oxidation process to form a 17-electron cation. At room temperature *fac*-$Cr(CO)_3(\eta^3\text{-}P_2P')$ gives a single chemically reversible one-electron oxidation response, but as the temperature is lowered (conventional electrodes) or the scan rate increases (microelectrodes) the process splits into two responses. At still faster scan rates (microelectrodes) only one reversible response is observed. These observations are consistent with the square reaction scheme

but the kinetics of the isomerization steps are faster than in all other similar metal carbonyl systems previously studied. At room temperature the potential of the observed response is a function of $E^\circ_{fac^+/fac^0}$, $E^\circ_{mer^+/mer^0}$, K_{fac^+/mer^+}, and K_{fac^0/mer^0}. At low temperatures (conventional electrodes) or high scan rates (microelectrodes) the individual redox couples are observed. At the fastest scan rates the electrochemical experiment outruns the time scale of the $fac^+ \rightarrow mer^+$ isomerization so that only the fac^+/fac^0 couple is observed. Digital simulation of the voltammograms has allowed the determination of all the equilibrium and rate constants in the square scheme for the chromium and molybdenum compounds. Of particular interest is the fact that the equilibrium constant (K_{fac^+/mer^+}) only weakly favors mer^+ for chromium, is close to unity for molybdenum, and weakly favors fac^+ for tungsten. Normally the mer^+ isomer is heavily favored. Additionally, the kinetics of all the isomerization steps are much faster than for all the other group 6 metal carbonyl derivatives previously studied. The voltammetric oxidations of $Mo(CO)_3(\eta^3\text{-}P_2P')$ and $W(CO)_3(\eta^3\text{-}P_2P')$ at room temperature and slow scan rates are complicated by an additional nonisomerization chemical step after electron transfer. However, at faster scan rates (>5 V s^{-1}) the influence of the kinetics of this additional reaction is minimized and the systems then show behavior analogous to that of $Cr(CO)_3(\eta^3\text{-}P_2P')$, although all rate constants for all isomerization steps are even greater than for chromium. The unusual position of equilibria and the fast kinetics of the isomerization steps in these compounds are attributed to steric strains within the tridentate ligand in both isomeric forms of the complexes, which lead to a delicate structural energy balance being achieved in both oxidation states.

Introduction

Many studies on the rates and mechanisms of substitution reactions have been undertaken for 18- and 17-electron metal carbonyl complexes.[4] Specifically, isotopic substitution studies of carbonyl exchange reactions have been widely reported and generally show considerable enhancement of lability for the 17-electron systems. For example, the rate of CO substitution of $V(CO)_6$ (17-electron system) is 10^{10} times faster than the corresponding reaction for the isostructural and also neutral 18-electron $Cr(CO)_6$.[5] Extensive studies by Brown[6,7] and other workers[4] on a wide range of 17-electron systems have led to the general conclusion that 17-electron systems react much faster than the corresponding 18-electron systems. However, this conclusion is conditional upon the absence of overriding steric and electronic complications,[8-10] since Basolo and co-workers have pointed out[4] that in certain cases, where steric terms are operative, the 17- and 18-electron com-

(1) Deakin University.
(2) University of Melbourne.
(3) Permanent address: Department of Applied Science, Brookhaven National Laboratory, Upton, NY 11973. On leave at Deakin University as a Gordon Research Fellow, Oct–Dec 1989.
(4) Hallinan, N. C.; Morelli, G.; Basolo, F. *J. Am. Chem. Soc.* **1988**, *110*, 6585.
(5) Shi, Q.-Z.; Richmond, T. G.; Trogler, W. C.; Basolo, F. *J. Am. Chem. Soc.* **1982**, *104*, 4032.
(6) Brown, T. L. *Ann. N.Y. Acad. Sci.* **1980**, *333*, 80.
(7) Herrinton, T. R.; Brown, T. L. *J. Am. Chem. Soc.* **1985**, *107*, 5700.
(8) Ellis, J. E.; Faltynek, R. A.; Rochfort, G. L.; Stevens, R. E.; Zank, G. A. *Inorg. Chem.* **1980**, *19*, 1082.
(9) McCullen, S. B.; Walker, H. W.; Brown, T. L. *J. Am. Chem. Soc.* **1982**, *104*, 4007.
(10) Therien, M. J.; Ni, C. L.; Anson, F. C.; Osteryoung, J. G.; Trogler, W. C. *J. Am. Chem. Soc.* **1986**, *108*, 4037.

0276-7333/91/2310-3320$02.50/0

pounds may react at similar rates.[11]

Another kind of reaction that has been studied in both 17- and 18-electron metal carbonyl systems is isomerization.[12] Both *cis* → *trans* and *fac* → *mer* isomerizations are invariably much faster in 17-electron compounds than in the 18-electron analogues and in the 17-electron case are generally unidirectional (see for example refs 13 and 14). Mingos[15] has shown that the electronic preference for a particular isomer switches from *cis* (or *fac*) to *trans* (or *mer*) in the 18- and 17-electron species, respectively. Thus, in the 17-electron systems both steric and electronic factors favor *trans* (or *mer*) compared with the usually competing influences of steric and electronic factors in the 18-electron systems. As a consequence, in electrochemical terms the oxidation of a facial 18-electron compound usually occurs as in eq 1, with the isomerization step

$$fac^0 \underset{+e^-}{\overset{-e^-}{\rightleftharpoons}} fac^+ \xrightarrow{k_{fac^+\rightarrow mer^+}} mer^+ \qquad (1)$$

following electron transfer normally being irreversible and the equilibrium for the $fac^+ \rightleftharpoons mer^+$ reaction heavily favoring the mer^+ isomer. Furthermore $k_{fac^+\rightarrow mer^+}$ is usually much faster than the corresponding step ($k_{fac^0\rightarrow mer^0}$) in an 18-electron system (eq 2).

$$fac^0 \xrightarrow{k_{fac^0\rightarrow mer^0}} mer^0 \qquad (2)$$

As in the case of the substitution reactions, it is possible that steric effects may, in certain circumstances, affect the rates of isomerization of metal carbonyl systems and modify the general conclusions reached in earlier studies. In this paper we present a spectroscopic and electrochemical study of the sterically constrained facial and meridional [M(CO)$_3$(η^3-P$_2$P′)]$^+$/M(CO)$_3$(η^3-P$_2$P′) redox couples (where M = Cr, Mo, W; P$_2$P′ = $Ph_2PCH_2CH_2P(Ph)CH_2CH_2PPh_2$), which display unusual isomeric lability in both oxidation states and, as a result, do not conform to eqs 1 and 2 under conventional electrochemical conditions. In addition, these systems provide the first example where the 17-electron fac^+ isomer is thermodynamically favored over the mer^+ isomer.

Experimental Section

The ligand P$_2$P′ was obtained from Strem Chemicals and was dried in a desiccator. The complex Cr(CO)$_3$(η^3-P$_2$P′) was prepared as described in the literature,[16] but the corresponding molybdenum and tungsten complexes were best prepared by an adaptation of the borohydride method.[17] M(CO)$_6$ (M = Mo, W) (1 mM) was refluxed under nitrogen in methylated spirits in the presence of $NaBH_4$ (2.5 mM) and P$_2$P′ (1 mM) for 5 h. The reaction was monitored by IR spectroscopy in the carbonyl region. The mixture was stirred overnight at room temperature; the solid product was filtered off and recrystallized from dichloromethane/*n*-hexane.

Conventional cyclic voltammograms were recorded in dichloromethane (0.1 M Bu_4NClO_4) with an EG&G PAR Model 174A polarographic analyzer. A three-electrode system was used with a platinum disk working electrode (radius 0.9 mm) and a platinum wire auxiliary electrode. The reference electrode was Ag/AgCl (CH_2Cl_2; saturated LiCl) and was separated from the test solution by a salt bridge containing 0.1 M Bu_4NClO_4 in CH_2Cl_2. For variable-temperature cyclic voltammetry, the temperature was regulated over the range +25 to −65 °C by using a dry-ice/acetone bath and the temperature was monitored with an alcohol thermometer. For rotating platinum disk experiments, a Beckman Model 1885 rotating platinum disk electrode (radius 3 mm) was used at a rotation rate of 2000 rpm with the same auxiliary and reference electrodes as above. Staircase cyclic voltammograms were obtained in dichloromethane (0.1 M Bu_4NBF_4) at the 0.9-mm-radius electrode by using a BAS 100A electrochemical analyzer.

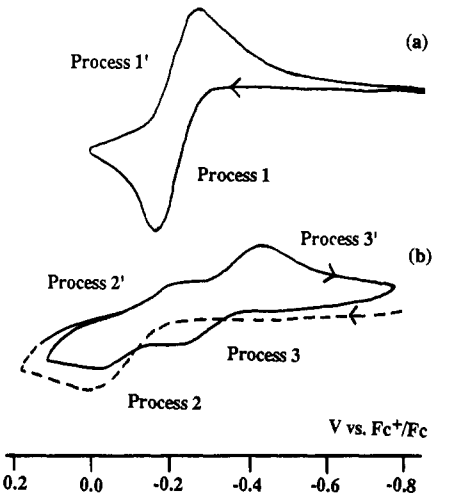

Figure 1. Oxidative cyclic voltammograms obtained at a conventional platinum disk electrode (radius 0.9 mm) for a 1 × 10^{-3} M solution of *fac*-Cr(CO)$_3$(η^3-P$_2$P′) in dichloromethane (0.1 M Bu_4NClO_4) with a scan rate of 0.1 V s^{-1}: (a) at 20 °C; (b) −45 °C (- - - is first scan).

All microelectrode electrochemical experiments were performed in dichloromethane (0.5 M Bu_4NBF_4) with a two-electrode cell arrangement as the low currents generated meant that potentiostatic control was not required.[18] A platinum wire pseudo reference electrode was used for fast-scan experiments at microelectrodes, as the internal resistance of a conventional reference electrode leads to distortion of the voltammograms. A PAR Model 175 function generator was used to provide wave forms, and the current was measured by a current follower based on an OPA 404 operational amplifier with variable gain (10^5–10^7 V A^{-1}). The voltage signal was then sent to a Gould Model 4035 digital storage oscilloscope and could then be transferred to an X–Y recorder or IBM personal computer via an IEEE 488 general-purpose interface bus.

The reversible redox couple Fc$^+$/Fc (Fc = $(C_5H_5)_2Fe$) was frequently measured to check the stability of the reference electrodes, and all results are quoted against this reference.

Phosphorus-31 NMR spectra were recorded by using a JEOL FX 100 spectrometer at 40.32 MHz, and chemical shifts were referenced against 85% H_3PO_4 with use of the high-frequency-positive sign convention. Infrared spectra were recorded on a Jasco A-302 spectrophotometer and calibrated against polystyrene (1601 cm^{-1}).

Results

The tritertiary phosphine $Ph_2PCH_2CH_2P(Ph)CH_2CH_2PPh_2$ (P$_2$P′) was first prepared by Chatt and Hart in 1960.[19] The group 6 metal tricarbonyl derivatives *fac*-M(CO)$_3$(η^3-P$_2$P′) have previously been prepared and characterized, including infrared and phosphorus-31 NMR spectroscopic studies, by other workers,[16] and our observed spectra agree with published data. The structures of *fac*-Cr(CO)$_3$(η^3-P$_2$P′) and *fac*-Mo(CO)$_3$(η^3-P$_2$P′) have also

(11) Freeman, J. W.; Wilson, D. R.; Ernst, R. D.; Smith, P. B.; Klendworth, D. D.; McDaniel, M. P. *J. Polym. Sci., Polym. Chem. Ed.* **1987**, *25*, 2063.
(12) Geiger, W. E. *Prog. Inorg. Chem.* **1985**, *33*, 275.
(13) Bond, A. M.; Colton, R.; McCormick, M. J. *Inorg. Chem.* **1977**, *16*, 155.
(14) Bond, A. M.; Colton, R.; Jackowski, J. J. *Inorg. Chem.* **1975**, *14*, 274.
(15) Mingos, D. M. P. *J. Organomet. Chem.* **1979**, *179*, C29.
(16) (a) Chatt, J.; Watson, H. R. *J. Chem. Soc.* **1961**, 4980. (b) King, R. B.; Kapoor, P. N.; Kapoor, R. N. *Inorg. Chem.* **1971**, *10*, 1841. (c) King, R. B.; Cloyd, J. C. *Inorg. Chem.* **1975**, *14*, 1550.
(17) Chatt, J.; Leigh, G. J.; Thankarajan, N. *J. Organomet. Chem.* **1971**, *29*, 105.
(18) Bixler, J. W.; Bond, A. M.; Lay, P. A.; Thorman, W.; van Den Bosch, P.; Fleischmann, M.; Pons, B. S. *Anal. Chim. Acta* **1986**, *187*, 67.
(19) Chatt, J.; Hart, F. A. *J. Chem. Soc.* **1960**, 1378.

been confirmed in the solid state by X-ray crystallography.[20]

A. Cyclic Voltammetric Oxidation of $Cr(CO)_3(\eta^3\text{-}P_2P')$ at Platinum Electrodes in Dichloromethane Solution. (i) Conventional Scan Rates and Electrodes. Scan rates of up to 0.5 V s^{-1} and disk electrodes of radius on the order of 1 mm are referred to as conventional conditions for cyclic voltammetry. Under these circumstances the mass transport to the electrode occurs essentially by linear diffusion.[21] Almost all previously reported metal carbonyl electrochemistry has been conducted under conventional conditions. The results of linear sweep and staircase voltammetry obtained in this work are essentially the same and are not distinguished in subsequent discussions.

Figure 1a shows a cyclic voltammogram for the oxidation of *fac*-$Cr(CO)_3(\eta^3\text{-}P_2P')$ at a scan rate of 0.1 V s^{-1} at 20 °C. Under these conditions a single chemically reversible diffusion controlled redox process is observed at around −0.1 V vs Fc^+/Fc (labeled process 1). This was shown to be a one-electron process by using rotating disk voltammetry and comparing the diffusion current with that generated by the known one-electron oxidation of an equimolar solution of *mer*-$Cr(CO)_3(\eta^1\text{-dpm})(\eta^2\text{-dpm})$.[22] There is also a second irreversible one-electron oxidation response (not shown) at more positive potential (peak potential about +0.7 V vs Fc^+/Fc). This second response remains irreversible under all conditions of temperature examined, and at faster scan rates its potential becomes still more positive until it eventually merges with the solvent background. This process is assigned to a further oxidation resulting in a very unstable Cr(II) carbonyl species and will not be considered further.

Since spectroscopic measurements (^{31}P NMR and IR) show that the compound exists in dichloromethane (0.1 M Bu_4NClO_4) as the *fac* isomer, an obvious interpretation of the voltammogram would be that process 1 is due to the simple reversible oxidation of the fac^0 isomer to the fac^+ isomer (eq 3); that is, a fac^+ isomer which is stable on the

$$fac\text{-}Cr(CO)_3(\eta^3\text{-}P_2P') \rightleftharpoons fac\text{-}[Cr(CO)_3(\eta^3\text{-}P_2P')]^+ + e^- \quad (3)$$

voltammetric time scale at room temperature is formed without the occurrence of the more usual isomerization depicted in eq 1. However, as the temperature is lowered (Figure 1b), the electrochemistry becomes more complex. On the first oxidation scan a single response is observed, and on the reverse reductive scan two waves are seen instead of only one. Moreover, on the second oxidation scan an additional response is seen and on all subsequent scans all four responses are observed. It is apparent that process 1 at room temperature has split into two reversible processes labeled 2,2′ and 3,3′ at −45 °C. This type of behavior is highly unusual in metal carbonyl chemistry, but there are precedents in organic electrochemistry which involve conformational processes undergoing rapid equilibria at room temperature that become slow on the electrochemical time scale at low temperature.[23] The temperature dependence suggests a new type of experimental observation for metal carbonyl complexes based upon the well-known

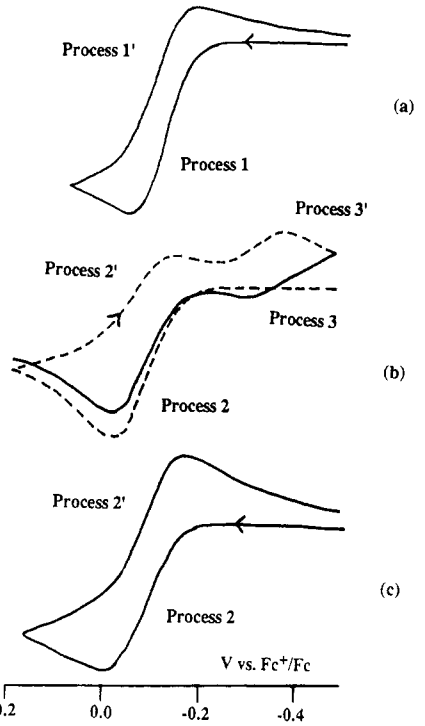

Figure 2. Oxidative cyclic voltammograms (20 °C) obtained at a platinum microdisk electrode (radius 25 μm) for a 1×10^{-3} M solution of *fac*-$Cr(CO)_3(\eta^3\text{-}P_2P')$ in dichloromethane (0.5 M Bu_4NBF_4): (a) scan rate 0.2 V s^{-1}; (b) scan rate 50 V s^{-1} (- - - is first scan); (c) scan rate 2000 V s^{-1}.

square reaction scheme shown in eq 4,[12-14] in which the $fac^+ \rightleftharpoons mer^+$ isomerization step is in rapid equilibrium under conventional conditions at room temperature, similar to the case of the *cis*-/*trans*-$[Cr(CO)_4(P\{OMe\}_3)_2]^+/Cr(CO)_3(P\{OMe\}_3)_2$ system.[24] At low temperatures the av-

$$\begin{array}{ccc} fac^0 & \rightleftharpoons & fac^+ + e^- \\ k_{mer^0 \rightarrow fac^0} \Big\uparrow \Big\downarrow k_{fac^0 \rightarrow mer^0} & & k_{mer^+ \rightarrow fac^+} \Big\uparrow \Big\downarrow k_{fac^+ \rightarrow mer^+} \\ mer^0 & \rightleftharpoons & mer^+ + e^- \end{array} \quad (4)$$

erage of the peak potentials at which processes 2 and 2′ are observed approximates the $E^\circ_{fac^+/fac^0}$ value and the average of the peak potentials, at which processes 3 and 3′ are observed, approximates the $E^\circ_{mer^+/mer^0}$ value. However, at room temperature the 17-electron $fac^+ \rightleftharpoons mer^+$ isomerization equilibrium is established so rapidly that on the conventional voltammetric time scale the effective E°_K (approximated by the average of the peak potential for processes 1 and 1′) is a function (which we will discuss shortly) of $E^\circ_{fac^+/fac^0}$, $E^\circ_{mer^+/mer^0}$, K_{fac^+/mer^+}, and K_{fac^0/mer^0}. That is, at room temperature the voltammetry may be explained by an equilibrium square scheme, the theory of which has been discussed in detail by Bond and Oldham.[25] A proven example of exchange averaging of electrochemical responses has been reported[24] in the $Cr(CO)_4(P\{OMe\}_3)_2$ system, but in that case the 17-electron equilibrium was still established rapidly on the voltammetric time scale at low temperatures, so that the individual $trans^+/trans^0$ and cis^+/cis^0 redox responses were not observed.

To further test the suggestion that eq 4 is operative, it is necessary to reduce the time scale of the electrochemical

(20) Favas, M. C.; Kepert, D. L.; Skelton, B. W.; White, A. H. *J. Chem. Soc., Dalton Trans.* **1980**, 447.
(21) Bond, A. M.; Oldham, K. B.; Zoski, C. G. *Anal. Chim. Acta* **1989**, *216*, 177.
(22) Bond, A. M.; Colton, R.; McGregor, K. *Inorg. Chem.* **1986**, *25*, 2378.
(23) (a) Evans, D. H., O'Connell, K. M. In *Electroanalytical Chemistry-A Series of Advances*; Bard, A. J., Ed.; Dekker: New York, 1986; Vol. 14, p 113. (b) Evans, D. H. *Chem. Rev.* **1990**, *90*, 739.
(24) Bond, A. M.; Colton, R.; Mann, T. F. *Organometallics* **1988**, *7*, 2224.
(25) (a) Bond, A. M.; Oldham, K. B. *J. Phys. Chem.* **1983**, *87*, 2492. (b) Bond, A. M.; Oldham, K. B. *J. Phys. Chem.* **1985**, *89*, 3739.

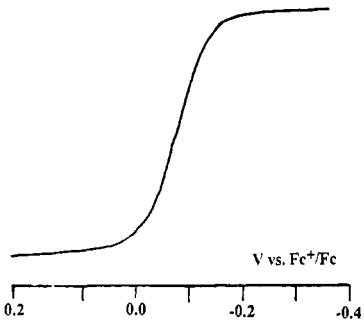

Figure 3. Steady-state oxidative cyclic voltammograms at a platinum microdisk electrode (radius 5 μm) for a 1 × 10^{-3} M solution of *fac*-Cr(CO)$_3$(η^3-P$_2$P′) in dichloromethane (0.5 M Bu$_4$NBF$_4$) with a scan rate of 0.01 V s^{-1}.

experiment in order to perturb the equilibria. Since dichloromethane is a high-resistance solvent, microelectrodes and high electrolyte concentrations are used to minimize the Ohmic *iR* drop.[21]

(ii) Microelectrodes. Microdisk electrodes may have a considerable component of radial diffusion, with the proportion relative to linear diffusion being dependent upon the scan rate and the radius of the electrode.[21]

Figure 2 shows oxidative cyclic voltammograms at 20 °C for a solution of *fac*-Cr(CO)$_3$(η^3-P$_2$P′) over the potential range −0.5 to +0.2 V vs Fc$^+$/Fc at a platinum microelectrode (radius 25 μm) as a function of scan rate. Under conditions relevant to Figure 1 a peak-shaped voltammetric curve is obtained with mass transport predominantly by linear diffusion.[21] At low scan rates with the 25-μm-radius electrode a single response (process 1) is observed; at intermediate scan rates two well-defined chemically reversible redox processes are observed (processes 2,2′ and 3,3′). These two stages are analogous to the room-temperature and low-temperature behavior shown in Figure 1. However, at very fast scan rates (≥1000 V s^{-1}) the response is a single chemically reversible couple (process 2,2′). Thus, by an increase in the scan rate, the observed response varies from one couple (slow scan rates) to two reversible couples (intermediate scan rates) and finally back to one reversible couple (very fast scan rates). In the previously described variable-temperature experiments at conventional electrodes and conventional scan rates, the return to a single reversible response was not observed, presumably because a sufficiently low temperature could not be achieved.

The data obtained with variable scan rates at the 25-μm-radius platinum disk microelectrode can be interpreted as follows. At very slow scan rates (Figure 2a) equilibria are maintained for the *fac*^{0}/*mer*^{0} and *fac*$^+$/*mer*$^+$ reactions and a single E°_K is observed. At intermediate scan rates (Figure 2b), where processes 2,2′ and 3,3′ are observable, approximate $E^\circ_{fac^+/fac^0}$ and $E^\circ_{mer^+/mer^0}$ values can be obtained. At very fast scan rates the time scale of the electrochemical experiment outruns the various kinetic steps in the square reaction scheme (eq 4) so that the system simplifies to the true *fac*$^+$/*fac*^{0} couple whose $E^\circ_{fac^+/fac^0}$ value can be measured directly from the voltammogram (Figure 2c). The postulate of isomerization occurring after electron transfer is based on analogy with many previously studied systems. It is supported by the fact that the separation of $E^\circ_{fac^+/fac^0}$ and $E^\circ_{mer^+/mer^0}$ is as expected.[12,13,22]

Figure 3 shows a cyclic voltammogram at a scan rate of 0.01 V s^{-1} for the oxidation of *fac*-Cr(CO)$_3$(η^3-P$_2$P′) with a smaller microelectrode (radius 5 μm) over the potential range at which process 1 occurs in dichloromethane (0.1 M Bu$_4$NBF$_4$). Radial-diffusion terms are now dominant, so a sigmoidal response rather than a peak is observed, indicating that steady-state conditions prevail.[21] A plot of E vs log $(i_d - i)/i$ is linear with a Nernstian slope of $2.303RT/nF$, and the $E_{1/2}$ value approximates to the E° value for the *fac*$^+$/*fac*^{0} redox couple (process 2). This is because the influence of chemical reactions following the electron-transfer step is decreased under these steady-state conditions.[21]

At extreme scan rates (very fast or very slow) kinetic factors are not important to a theoretical understanding of the cyclic voltammetry under conditions where linear diffusion is the dominant mode of mass transport. With use of data obtained from the limiting cases, a thermodynamic description of the square reaction scheme is possible. Reference 26 contains a derivation of theory applicable to the equilibrium situation. The equations relevant to this work are

$$E^\circ_K = E^\circ_{mer^+/mer^0} - \frac{RT}{F} \ln \left[\frac{1 + K_{fac^+/mer^+}}{1 + K_{fac^0/mer^0}} \right] \quad (5)$$

$$E^\circ_K = E^\circ_{fac^+/fac^0} + \frac{RT}{F} \ln \left[\left(1 + \frac{1}{K_{fac^0/mer^0}} \right) \Big/ \left(1 + \frac{1}{K_{fac^+/mer^+}} \right) \right] \quad (6)$$

where E°_K = equilibrium potential of the weighted average of the $E^\circ_{fac^+/fac^0}$ and $E^\circ_{mer^+/mer^0}$ values, $K_{fac^0/mer^0} = [fac^0]/[mer^0]$, and $K_{fac^+/mer^+} = [fac^+]/[mer^+]$.

The difference between $E^\circ_{fac^+/fac^0}$ and $E^\circ_{mer^+/mer^0}$ allows the equilibrium constant K_{CR} for the cross redox reaction

$$fac^+ + mer^0 \underset{}{\overset{K_{CR}}{\rightleftharpoons}} fac^0 + mer^+ \quad (7)$$

to be calculated where

$$K_{CR} = \frac{K_{fac^0/mer^0}}{K_{fac^+/mer^+}} \quad (8)$$

and

$$E^\circ_{fac^+/fac^0} - E^\circ_{mer^+/mer^0} = \frac{RT}{F} \ln K_{CR} \quad (9)$$

In order to obtain equilibrium and rate constants for the system, digital simulations of the square reaction scheme were undertaken for different scan rates with use of the Dufort–Frankel method[27] applied to a microdisk electrode, so that both the linear and radial diffusion components were included.[28] Experimental voltammograms were corrected for the charging current and Ohmic *iR* drop by methods that will be described elsewhere.[28] The kinetics of the second-order cross redox reaction in eq 8 were included in the simulation but were shown not to be important. As shown in Figure 4, the fit between experimental and simulated scans is excellent. The heterogeneous charge transfer rate constants (k_s values)[29] are large, and the charge transfer coefficients (α values)[29] are con-

(26) Laviron, E.; Roullier, L. *J. Electroanal. Chem. Interfacial Electrochem.* **1985**, *186*, 1.
(27) (a) Dufort, E. L.; Frankel, S. P. *Math. Tables Other Aids Comput.* **1953**, *43*, 135. (b) Marques da Silva, B.; Avaca, L. A.; Gonzalez, E. R. *J. Electroanal. Chem. Interfacial Electrochem.* **1989**, *269*, 1. (c) Gourlay, A. R. *J. Inst. Math. Its Appl.* **1970**, *6*, 375. (d) Feldberg, S W. *J. Electroanal. Chem. Interfacial Electrochem.* **1990**, *290*, 49. (e) Lerke, S. A.; Evans, D. H.; Feldberg, S. W. *J. Electroanal. Chem. Interfacial Electrochem.* **1990**, *296*, 299.
(28) Bond, A. M.; Colton, R.; Feldberg, S. W.; Greenhill, H. B.; Mahon, P. J.; Whyte, T. To be submitted for publication.
(29) Bard, A. J.; Faulkner, L. R. *Electrochemical Methods: Fundamentals and Applications*; Wiley: New York, 1980.

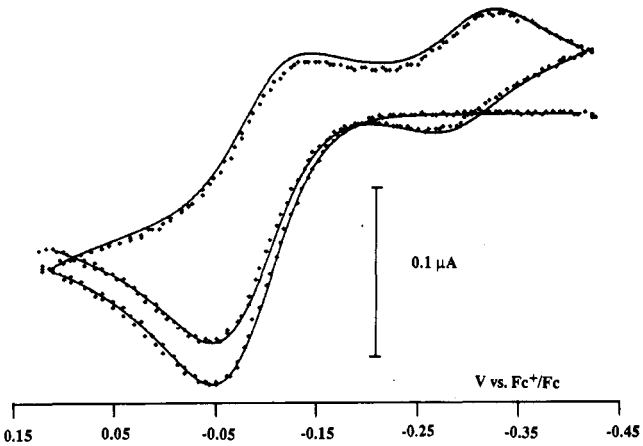

Figure 4. Comparison between experimental (crosses) and simulated (solid line) oxidative cyclic voltammograms (20 °C) obtained at a platinum microdisk electrode (radius 25 μm) for a 1 × 10^{-3} M solution of *fac*-$Cr(CO)_3(\eta^3\text{-}P_2P')$ in dichloromethane (0.5 M Bu_4NBF_4) with a scan rate of 50 V s^{-1}. See Table I for values of parameters.

Table I. Thermodynamic and Kinetic Data for the Redox Systems $[Cr(CO)_3(\eta^3\text{-}P_2P')]^+/Cr(CO)_3(\eta^3\text{-}P_2P')$, $[Cr(CO)_3(P\{OMe\}_3)_3]^+/Cr(CO)_3(P\{OMe\}_3)_3$, and $[Mo(CO)_3(\eta^3\text{-}P_2P')]^+/Mo(CO)_3(\eta^3\text{-}P_2P')$ in Dichloromethane

param	$Cr(CO)_3(\eta^3\text{-}P_2P')$ syst[a]	$Cr(CO)_3(P\{OMe\}_3)_3$ syst[b]	$Mo(CO)_3(\eta^3\text{-}P_2P')$ syst[a]
$E^\circ_{fac^+/fac^0}$, V vs Fc^+/Fc	−0.085	0.000	0.145
$E^\circ_{mer^+/mer^0}$, V vs Fc^+/Fc	−0.310	−0.13	−0.090
E_K, V vs Fc^+/Fc	−0.122		0.125
K_{fac^0/mer^0}	1.5 × 10^3	2.5 × 10^{-1}	1 × 10^4
K_{fac^+/mer^+}	3.1 × 10^{-1}	1.6 × 10^{-3}	9.1 × 10^{-1}
K_{CR}	5.0 × 10^3	1.6 × 10^2	1.1 × 10^4
$k_{fac^+\rightarrow mer^+}$, s^{-1}	5.0 × 10^2	1.1 × 10^{-1}	1.2 × 10^3
$k_{mer^+\rightarrow fac^+}$, s^{-1}	1.6 × 10^2	1.7 × 10^{-4}	1.1 × 10^3
$k_{fac^0\rightarrow mer^0}$, s^{-1}	5.0 × 10^{-2}	1.8 × 10^{-4}	1.0 × 10^{-1}
$k_{mer^0\rightarrow fac^0}$, s^{-1}	77	4.5 × 10^{-5}	1.0 × 10^3
$k_s(fac^+/fac^0)$, cm s^{-1} [c]	2.0 × 10^{-1}		1.5 × 10^{-1}
$k_s(mer^+/mer^0)$, cm s^{-1} [c]	3.0 × 10^{-1}		1.2 × 10^{-1}
$\alpha(fac^+/fac^0)$ [d]	0.30		0.40
$\alpha(mer^+/mer^0)$ [d]	0.45		0.45

[a] Data obtained at 20 °C with 0.5 M Bu_4NBF_4 as the electrolyte; diffusion coefficient assumed to be 6 × 10^{-6} cm^2 s^{-1} for all species. [b] Data obtained at 22 °C with 0.1 M Bu_4NClO_4 as the electrolyte; see ref 30 for details. [c] k_s is the rate of heterogeneous charge transfer at E°. [d] α is the charge-transfer coefficient.

siderably less than 0.5. If the electrode kinetics are ignored and the charge transfer process is assumed to be Nernstian, the agreement between simulations and experimental curves is not so good.

Table I summarizes the equilibrium and rate constants calculated from the comparison of simulated and experimental data for the $[Cr(CO)_3(\eta^3\text{-}P_2P')]^+/Cr(CO)_3(\eta^3\text{-}P_2P')$ redox system square reaction scheme shown in eq 4 together with electrode kinetic data. The values obtained for the thermodynamic parameters via the simulations conform closely to the values obtained by the calculation based on the limiting situations where chemically reversible data are obtained. For comparison purposes Table I also includes data for the $Cr(CO)_3(P\{OMe\}_3)_3$ system,[30] which exhibits typical behavior in the context of the relative stability of the various isomers in the square reaction scheme.

The equilibrium constant K_{fac^+/mer^+} for $Cr(CO)_3(\eta^3\text{-}P_2P')$ only slightly favors the mer^+ isomer ($K_{fac^+/mer^+} \approx 0.31$),

(30) Bond, A. M.; Colton, R.; Kevekordes, J. E. *Inorg. Chem.* **1986**, *25*, 749.

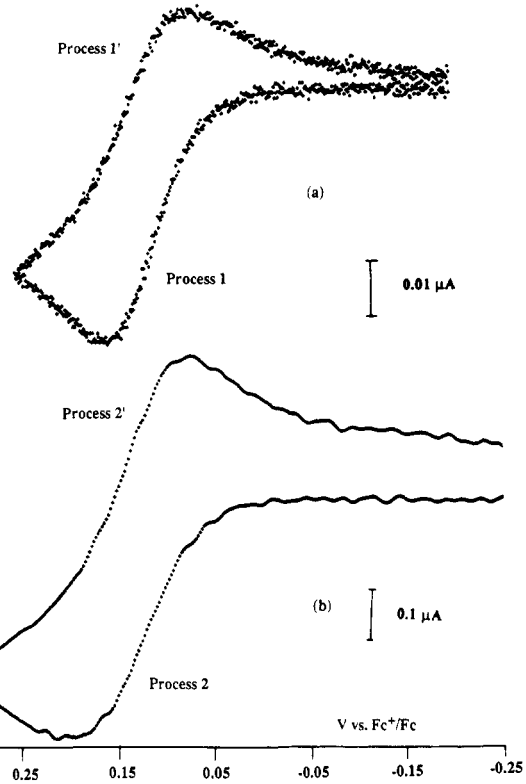

Figure 5. Oxidative cyclic voltammograms (20 °C) obtained at a platinum microelectrode (radius 25 μm) for a 1 × 10^{-3} M solution of *fac*-$Mo(CO)_3(\eta^3\text{-}P_2P')$ in dichloromethane (0.5 M Bu_4NBF_4): (a) scan rate 5 V s^{-1}; (b) scan rate 2000 V s^{-1}.

whereas in previously studied systems the mer^+ isomer is strongly favored.[12-14,29] Additionally the back reaction $mer^+ \rightarrow fac^+$ ($k_{mer^+\rightarrow fac^+} \approx 1.6 \times 10^2$) is many orders of magnitude faster than usual (Table I). In the fac^0/mer^0 pair of isomers the equilibrium constant heavily favors the fac^0 isomer, but the unusual feature is that the rates of both the forward and reverse isomerization reactions are sufficiently fast to influence the cyclic voltammograms obtained at conventional scan rates.

B. Cyclic Voltammetric Oxidation of $Mo(CO)_3(\eta^3\text{-}P_2P')$ at Platinum Electrodes in Dichloromethane Solution. (i) Conventional Scan Rates and Electrodes. At conventional scan rates and electrode sizes the molybdenum complex gives an initial two-electron irreversible oxidation process at a potential of about +0.1 V vs Fc^+/Fc, which remains chemically irreversible regardless of the switching potential, at temperatures down to −65 °C. This is followed at more positive potentials and also on the reverse scan by a series of processes that are not relevant to the theme of this paper. Rotating disk voltammetry shows the limiting current for the initial process to be approximately twice that for oxidation of an equimolar solution of $Cr(CO)_3(\eta^1\text{-dpm})(\eta^2\text{-dpm})$, which has a known one-electron oxidation.[22] The electrochemical reversibility of the first electron transfer step, which is of interest in the present study, is implied in the shape of the voltammogram. The observation of the chemically irreversible two-electron process implies the existence of a chemical step (nonisomerization) following the initial electron transfer. This nonisomerization chemical step produces electroactive species and occurs in competition with the isomerization reaction.

(ii) Microelectrodes. Figure 5 shows cyclic voltammograms for $Mo(CO)_3(\eta^3\text{-}P_2P')$ at scan rates of 5 and 2000 V s^{-1} at a platinum microdisk electrode of radius 25 μm, while Figure 6 shows the response at a scan rate of 200 V

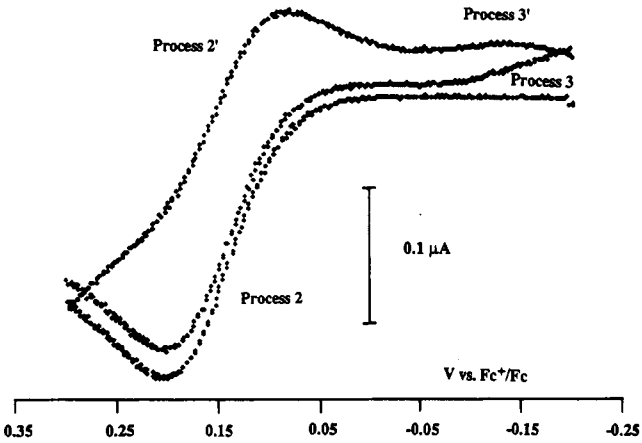

Figure 6. Oxidative cyclic voltammograms (20 °C) obtained at a platinum microelectrode (radius 25 μm) for a 1×10^{-3} M solution of *fac*-Mo(CO)$_3$(η^3-P$_2$P′) in dichloromethane (0.5 M Bu_4NBF_4) at a scan rate of 200 V s^{-1}.

s^{-1}. At scan rates greater than 5 V s^{-1} the influence of the chemical reaction (not isomerization) following the first electron transfer step is minimized on the short time scale of this experiment and the process reverts to an overall one-electron rather than a two-electron process.

At a scan rate of 5 V s^{-1} (Figure 5a) the redox process now appears to be a chemically reversible one-electron step, process 1,1′ (eq 10), analogous to that observed for Cr(CO)$_3$(η^3-P$_2$P′) at a scan rate of 0.2 V s^{-1} (Figure 2a). As

$$\text{Mo(CO)}_3(\eta^3\text{-P}_2\text{P}') \rightleftharpoons [\text{Mo(CO)}_3(\eta^3\text{-P}_2\text{P}')]^+ + e^- \quad (10)$$

the scan rate is increased to 200 V s^{-1}, the apparently simple one-electron process is split into processes 2,2′ and 3,3′ (Figure 6) corresponding to the presence of the square reaction scheme (eq 4). At very fast scan rates (≥2000 V s^{-1}) a single one-electron response, process 2,2′, corresponding to the *fac*$^+$/*fac*^{0} couple for the oxidation of *fac*-Mo(CO)$_3$(η^3-P$_2$P′) is observed (Figure 5b). That is, once a sufficiently short time scale is achieved to avoid the influence of the nonisomerization chemical step, then the system is similar to that of its chromium analogue. However, for molybdenum much faster scan rates are required to achieve the chemically reversible *fac*$^+$/*fac*^{0} redox couple (compare Figures 2 and 5).

Results of calculations based on the limiting cases of chemically reversible data obtained at fast and slow scan rates and digital simulations of the electrochemistry for the molybdenum system are contained in Table I. All the rate constants are much faster than for chromium. The *mer*$^+$/*mer*^{0} response (Figure 6) is not as well pronounced as in the chromium case (Figures 2 and 4), so that the values for $E^\circ_{mer^+/mer^0}$, K_{fac^0/mer^0}, K_{CR}, $k_{fac^0\rightarrow mer^0}$, and $k_{mer^0\rightarrow fac^0}$ are relatively imprecise. However, it is still possible to calculate K_{fac^+/mer^+} accurately because its value is derived from E°_K and $E^\circ_{fac^+/fac^0}$, both of which can be precisely determined. The value of K_{fac^+/mer^+} is 0.91, which indicates that the *mer*$^+$ isomer is the slightly thermodynamically favored isomer. The value of 0.91 is consistent with the difficulty in observing a well-defined *mer*$^+$ + e$^-$ → *mer*^{0} response under any conditions of scan rate since the concentration of *mer*$^+$ at the electrode surface can never be high.

C. Cyclic Voltammetric Oxidation of W(CO)$_3$(η^3-P$_2$P′) at Platinum Electrodes in Dichloromethane. (i) Conventional Scan Rates and Electrodes. Under conventional conditions W(CO)$_3$(η^3-P$_2$P′) displays a chemically irreversible oxidation response at about +0.09 V vs Fc$^+$/Fc with additional small responses at more positive potentials and also on the reverse scan similar to those observed for Mo(CO)$_3$(η^3-P$_2$P′).

(ii) Microelectrodes. As with the molybdenum complex, by use of a microelectrode and fast scan rates or low temperatures, the influence of nonisomerization chemical reaction following electron transfer can be minimized. The voltammetry at fast scan rates in the tungsten system is similar to that in the molybdenum case, although conditions could not be achieved when the *mer*$^+$/*mer*^{0} couple can be clearly observed above background with use of scan rates up to 8000 V s^{-1}. With the sparingly soluble *fac*-W(CO)$_3$(η^3-P$_2$P′) (saturated solution $<1 \times 10^{-3}$ M) it is not at present possible in dichloromethane to use higher scan rates with adequate charging current and Ohmic *iR* drop corrections. However, it could be shown that the tungsten system provides the first case where the *fac*$^+$ isomer is the thermodynamically preferred isomer in a 17-electron metal carbonyl system. That is, the value of K_{fac^+/mer^+} is greater than 1, but because of experimental and theoretical limitations for this system neither this nor other thermodynamic parameters can be determined accurately. For the tungsten system, the square scheme essentially reduces to a reversible *fac*^{0} ⇌ *fac*$^+$ + e$^-$ redox process under the fast scan rate voltammetric conditions employed in this work with a potential which is similar to that of the molybdenum analogue.

General Discussion

Structural Effects. The thermodynamics of these M(CO)$_3$(η^3-P$_2$P′) systems are not unusual in the sense that the E° values of the two isomeric redox couples and their difference in potential are typical for group 6 metal tricarbonyl complexes.[22] The unusual feature of these systems is that all the rate constants are much greater than is usual for other tricarbonyl systems. In particular the *mer*$^+$ → *fac*$^+$ isomerization, which normally does not influence electrochemical measurements, is much faster than usual and is significant on the voltammetric time scale in the [M(CO)$_3$(η^3-P$_2$P′)]$^+$/M(CO)$_3$(η^3-P$_2$P′) systems. Additionally, the equilibrium constant K_{fac^+/mer^+}, which usually heavily favors the *mer*$^+$ isomer ($K_{fac^+/mer^+} \ll 1$), is now delicately balanced around the value $K_{fac^+/mer^+} \approx 1$ and actually favors the *fac*$^+$ isomer for tungsten ($K_{fac^+/mer^+} > 1$). Although the tungsten case provides the first example where the *fac*$^+$ isomer is preferred in the 17-electron cation, the values of K_{fac^+/mer^+} are in fact quite similar in all three cases but with a definite trend in the sequence from chromium to molybdenum to tungsten. While our data appear to be unique with respect to metal tricarbonyl chemistry, an analogous situation may apply to *cis*$^+$/*trans*$^+$ isomerization in the [Mo(CO)$_4$(carbene)$_2$]$^+$ system, where the unusual situation of the *cis*$^+$ isomer being favored over the *trans*$^+$ isomer has been reported.[31]

We believe that in the case of the M(CO)$_3$(η^3-P$_2$P′) complexes, but not in previously studied tricarbonyl systems, there are significant steric pressures in *both* the *fac* and *mer* isomers which are delicately balanced with the well-known electronic preferences for particular isomers in each oxidation state.[15] Molecular models based on the known crystal structures[20] of both *fac*-Cr(CO)$_3$(η^3-P$_2$P′) and *fac*-Mo(CO)$_3$(η^3-P$_2$P′) indicate that in the *fac* geometry there is a substantial interaction between a phenyl group of each of the two terminal diphenylphosphino groups unless the phenyl rings are parallel. This steric interaction was discussed in the crystallographic paper.[20] In the solid state these phenyl rings are indeed roughly parallel,

(31) Rieke, R. D.; Kojima, H.; Ofele, K. *J. Am. Chem. Soc.* **1976**, *98*, 6735.

thereby minimizing this interaction, but in solution the phenyl rings would normally rotate and this leads to even greater interaction. With use of the same bond distances for the *mer* isomer as those found for the *fac* isomer, molecular models show that this particular steric effect is completely absent in the *mer* isomer, but instead there is considerable strain in the formation of the two five-membered chelate rings, which originates in the unfavorable angles at the central phosphorus atom. The complexes are therefore subject to strain in both configurations and are not completely stable in either isomeric form for either the 18- or 17-electron configurations. For the present complexes in the 17-electron state these influences reveal themselves in both kinetic and thermodynamic effects, and they rapidly interconvert between the two highly strained isomeric structures. The effect of replacing three monodentate ligands with the tridentate P_2P' ligand is to increase the value of K_{fac^+/mer^+} by several orders of magnitude (Table I). However, the variation in K_{fac^+/mer^+} upon changing the metal is relatively small.

Acknowledgment. S.W.F. thanks the Deakin University Research Committee for the award of a Gordon Fellowship during a 1989 sabbatical leave. Support of the U.S. Department of Energy, under Contract No. DE-AC0276CH00016, is gratefully acknowledged. P.M. and T.W. thank the Australian Government for Postgraduate Research Awards. Funding provided by the Australian Research Council is also gratefully acknowledged.

Oxygen- and Carbon-Bound Ruthenium Enolates: Migratory Insertion, Reductive Elimination, β-Hydrogen Elimination, and Cyclometalation Reactions

John F. Hartwig, Robert G. Bergman,* and Richard A. Andersen*

Department of Chemistry, University of California, Berkeley, California 94720

Received March 26, 1991

The generation of a series of reactive ruthenium complexes of the general formula $(PMe_3)_4Ru(R)(enolate)$ is reported. Most of these enolates have been shown to bind to the ruthenium center through the oxygen atom. This binding mode is evident from solution NMR data as well as from an X-ray crystal structure of a representative example. Two of the enolate complexes **8** and **9** exist in equilibrium between the O- and C-bound forms; both isomers can be identified clearly by NMR spectroscopy. Variable-temperature NMR studies demonstrate that the ratio of the two isomers changes reversibly with temperature, demonstrating that it represents the equilibrium distribution. Synthesis of the bulky ruthenium enolate **10** results in dissociation of phosphine and formation of a complex in which the enolate hydrogen is coordinated to the metal center in an agostic binding mode. X-ray structural analysis demonstrates that the complex contains one Ru–O bond and one agostic interaction between the ruthenium center and the vinylic hydrogen. The reactions of these compounds include the β-migration of the phenyl group in $(PMe_3)_4Ru(Ph)(OC(CH_2)Me)$ (**4a**) to form oxametallacyclobutane $(PMe_3)_4Ru(OC(Me)(Ph)CH_2)$ (**11**). Heating $(PMe_3)_4Ru(H)(OC(CH_2)Me)$ with CO at 85 °C for 8 h led to reductive elimination of acetone and formation of the Ru(0) complex $(PMe_3)_2Ru(CO)_3$. Warming a solution of $(PMe_3)_4Ru(Me)(OC(CH_2)Me)$ to 65 °C led to β-hydrogen elimination, forming $(PMe_3)_4Ru(Me)(H)$. This transformation constitutes the formal elimination of ketene, and when this thermolysis was run in the presence of tert-butyl alcohol as a trap, *tert*-butyl acetate was formed in 10–15% yield, consistent with the formation of ketene during the course of the reaction. Addition of the potassium enolate of acetaldehyde to phenyl chloride $(PMe_3)_4Ru(Ph)(Cl)$ (**1**) yielded $(PMe_3)_3(CO)Ru(Ph)(Me)$. A mechanism initiated by an analogous β-hydrogen elimination reaction is proposed. Other enolate complexes undergo cyclometallation reactions to form oxygen-containing metallacycles. Thermolysis of $(PMe_3)_4Ru(Me)(OC(CH_2)Me)$ (a mixture of O- and C-bound isomers **8a** and **8b**) forms the acetone dianion complex $(PMe_3)_4Ru((CH_2)_2CO)$ (**14**). Cyclometalation of $(PMe_3)_4Ru(Me)(OC(CH_2)CMe_3)$ (**5c**) led to formation of the oxametallacyclobutene complex $(PMe_3)_4Ru(OC(CMe_3)CH)$ (**16**). Addition of 2 equiv of potassium enolate to $(PMe_3)_4Ru(OAc)(Cl)$ (**12**) also led to metallacyclic products. Reaction of 2 equiv of the potassium enolate of acetone with **12** yielded **14**, while 2 equiv of the potassium enolate of 4,4-dimethyl-2-pentanone provided oxametallacyclobutane $(PMe_3)_4Ru(OC(=CHCMe_3)CH_2)$ (**13**).

Introduction

Until recently, the organometallic chemistry of late-transition-metal systems has focused on metal–carbon and –hydrogen bonds. Many routes to formation of metal alkyl, aryl, allyl, and hydride complexes have been investigated, and reactions such as β-hydrogen elimination, reductive elimination, and migratory insertion are well documented. The preparation and reactivity of compounds containing late transition-metal–oxygen bonds is less common. It has been proposed that combining a hard ligand with a soft late-metal center may lead to weak late-metal–heteroatom linkages and result in reactive late-metal–heteroatom bonds.[1]

Several research groups have been interested in transition-metal–enolate complexes from the perspective of using the metal center as a potential site of asymmetry in the design of chiral catalysts for aldol reactions. Indeed, transition-metal-mediated aldol reactions have been observed,[2] and some systems undergo catalytic aldol reac-

(1) (a) Bryndza, H. E.; Tam, W. *Chem. Rev.* **1988**, *88*, 1163 and references therein. (b) Pearson, R. G. *J. Am. Chem. Soc.* **1963**, *85*, 3533.

(2) (a) Mukaiyama, T.; Banno, K.; Narasaka, K. *J. Am. Chem. Soc.* **1974**, *96*, 7503. (b) Evans, D. A.; McGee, L. R. *Tetrahedron Lett.* **1980**, 3975. (c) Yamamoto, Y.; Naruyama, K. *Tetrahedron Lett.* **1980**, 4607. (d) Stille, J. R.; Grubbs, R. H. *J. Am. Chem. Soc.* **1983**, *105*, 1665. (e) Sato, S.; Matsuda, I.; Izumi, Y. *Tetrahedron Lett.* **1986**, 5517. (f) Reetz, M. T.; Vougioukas, A. E. *Tetrahedron Lett.* **1987**, *28*, 793.

0276-7333/91/2310-3326$02.50/0